Cell, Vol. 95, 993–1003, December 23, 1998, Copyright ©1998 by Cell Press

Procollagen Traverses the Golgi Stack without Leaving the Lumen of Cisternae: Evidence for Cisternal Maturation

Lidia Bonfanti,*†# Alexander A. Mironov, Jr.,*†# José A. Martínez-Menárguez,§ Oliviano Martella,*† Aurora Fusella,*† Massimiliano Baldassarre,*‡ Roberto Buccione,*‡ Hans J. Geuze,§ Alexander A. Mironov,*†‖ and Alberto Luini*‡‖

*Istituto di Ricerche Farmacologiche "Mario Negri"
Consorzio Mario Negri Sud
Department of Cell Biology and Oncology
†Unit of Morphology and
‡Laboratory of Molecular Neurobiology
66030 S. Maria Imbaro (Chieti)
Italy
§Department of Cell Biology
Medical School and Institute of Biomembranes
Utrecht University
3584CX Utrecht
The Netherlands

Summary

Newly synthesized procollagen type I (PC) assembles into 300 nm rigid, rod-like triple helices in the lumen of the endoplasmic reticulum. This oligomeric complex moves to the Golgi and forms large electron-dense aggregates. We have monitored the transport of PC along the secretory pathway. We show that PC moves across the Golgi stacks without ever leaving the lumen of the Golgi cisternae. During transport from the endoplasmic reticulum to the Golgi, PC is found within tubular-saccular structures greater than 300 nm in length. Thus, supermolecular cargoes such as PC do not utilize the conventional vesicle-mediated transport to traverse the Golgi stacks. Our results imply that PC moves in the anterograde direction across the Golgi complex by a process involving progressive maturation of Golgi cisternae.

Introduction

The Golgi complex receives secretory proteins from the endoplasmic reticulum (ER), transfers them through its own differentiated compartments, characteristically organized into stacks of flat cisternae, and distributes them to their final destinations. It is well documented that proteins arrive in the Golgi cisternae by carriers formed by the coat protein COPII (Rothman and Wieland, 1996; Schekman and Orci, 1996). The mode of protein traffic across the Golgi stack remains controversial, and all possible avenues have been documented or hypothesized. While it may turn out that small soluble and membrane proteins are carried across the Golgi stacks and in general along the secretory pathway by transport vesicles, the process by which large multimeric protein complexes, such as algal scales, procollagen (PC), and lipoprotein droplets, are transported remains largely unknown. In the latter case it has been suggested that transport occurs through progressive maturation of the Golgi cisternae (Mironov et al., 1997); however, there is no direct experimental evidence to support this scheme.

The cisternal maturation model dictates that cargo moves through the Golgi complex without leaving the cisternal lumen and that secretion occurs by progressive maturation of the Golgi cisternae as they move in the *cis-trans* direction. Cisternae-specific proteins such as glycosyltransferase are continuously retrieved by retrograde vesicles during this process (Bannykh and Balch, 1997; Mironov et al., 1997; Schekman and Mellman, 1997). This model does not present major theoretical problems; it is compatible with virtually all of the biochemical and genetic evidence gathered so far and appears to be better suited than vesicular transport to explain intra-Golgi traffic (Schekman and Mellman, 1997; Pelham, 1998). Among the numerous examples of supramolecular secretory complexes observed inside the Golgi cisternae are the casein submicelles in lactating mammary gland cells, PC aggregates in embryonic fibroblasts, large proteinaceous membrane thickenings in urothelial cells, and scales in scale-covered algae (see Mironov et al., 1997). These cargoes are much too large to be packaged into transport vesicles. However, as mentioned above and discussed recently, these observations do not provide direct and sufficient proof of the maturation mechanism (Schekman and Mellman, 1997). The presence of supramolecular cargoes in Golgi cisternae can be explained by modified versions of the vesicular shuttle model. First, it is possible that the large aggregates observed inside Golgi cisternae might disassemble into smaller subunits, enter transport vesicles, and subsequently reassemble in the acceptor cisterna. Second, cells secreting large supramolecular cargoes might induce the formation of secretory carriers of a size sufficient to accommodate large particles (this has been shown to occur, at least in the case of clathrin-coated vesicles; see Schmelz et al., 1994; Schekman and Mellman, 1997). Third, the cisternae containing supramolecular cargoes might in fact belong to the *trans*-Golgi network (TGN) and not earlier cisternae; this would not represent a departure from classical transport models because the formation of such cargoes in the TGN could be similar to granule condensation in regulated secretory systems. Fourth, the large intralumenal complexes might be stationary assemblies of secretory molecules without functional significance; these molecules might nonspecifically aggregate in Golgi cisternae whilst en route to the plasma membrane, with the specific and functionally relevant transport of proteins being carried by anterograde vesicles. These are obvious concerns that need to be addressed to demonstrate the existence of cisternal maturation as a bona fide mode of transport along the secretory pathway. However, this has been impossible so far because suitable experimental tools and cellular systems have been lacking.

‖To whom correspondence should be addressed (e-mail: mironov@cmns.mnegri.it or luini@cmns.mnegri.it).

#These authors contributed equally to this work.

The main requirement to test the maturation model is that the cargo being transported by cisternal maturation should possess a specific set of features: it should be of a size markedly larger than that of transport vesicles; it should have a molecular structure that precludes disassembly into smaller components that may be packaged into vesicles; it should be suitable for immunoelectron microscopy studies, as well as for biochemical quantitation of release; and it should be readily visualizable by electron microscopy. Finally, the movement of this cargo down the secretory system should be amenable to synchronization, much in the same way as transport of the temperature-sensitive VSV-G protein is synchronized using temperature shifts (Bergmann, 1989). We have searched for a suitable cargo and found that, among the known secretory supramolecular complexes, PC fits the above requirements.

We have monitored the transport of supramolecular aggregates of PC along the secretory pathway in embryonic tendon (ET) fibroblasts. Immunoelectron microscopy of serial sections of these cells reveals that upon arriving in the first cisternae of the Golgi stacks, the PC aggregates remain confined in the lumen of the cisternae. By following a synchronous wave of this migration, we find that PC aggregates move in the *cis-trans* direction without ever entering conventional small vesicles or larger dissociative elements. These findings imply that intracellular transport of PC occurs by cisternal maturation.

Results

Background

PC is a long (300 nm), rod-like (1.5 nm diameter) protein composed of three chains dominated by stretches of 1000 amino acids rich in proline and hydroxyproline (Bachinger et al., 1993). In the ER, these chains are packed into an uninterrupted triple helix that is stabilized by hydrogen bonds between all the residues in the chains. This results in a 300 nm long, rigid, rod-like structure (Brodsky and Ramshaw, 1997). Two globular propeptides situated at both the C- and N-terminal ends serve to align the chains in register for proper folding and are cleaved after secretion (Bachinger et al., 1993). The folding of the PC triple helix requires the hydroxylation of specific prolines by prolyl hydroxylase because hydroxyproline is essential in creating the stabilizing hydrogen bonds. If prolyl hydroxylase is inhibited, PC does not fold and is retained in the ER (Beck et al., 1996); however, PC refolds rapidly and exits the ER upon reactivation of prolyl hydroxylase (Sarras et al., 1991). Thus, by inhibiting and reactivating prolyl hydroxylase, the transport of PC through the secretory pathway can be synchronized. Once inside the Golgi complex, PC helices align side by side into large aggregates that appear as electron-dense material in micrographs (Trelstad and Hayashi, 1979; Leblond, 1989). We have used these properties of PC in combination with specific antibodies to monitor the transport of synchronized waves of PC along the secretory pathway by electron microscopy.

Structure and Localization of PC in the Secretory Pathway of ET Fibroblasts

The ultrastructure of the Golgi complex of PC-secreting odontoblasts, osteoblasts, and tendon fibroblasts has been thoroughly described before (Trelstad and Hayashi, 1979; Leblond, 1989). Its unique characteristic is the presence of expanded distensions continuous with Golgi cisternae, approximately 350 nm long and 150 nm thick, containing aggregates of laterally aligned PC triple helices. ET fibroblasts from chicken are a good model system for our study because they are efficient producers and secretors of PC (Trelstad and Hayashi, 1979) and can be isolated in large numbers in culture (Kao et al., 1977). When separated from tendon and kept in 1% adult bovine serum on a fibronectin-coated support, chick ET fibroblasts preserved a normal morphology (see Trelstad and Hayashi, 1979; Leblond, 1989) and a high rate of collagen secretion for up to 18 hr. Distensions averaged 319 ($\pm$ 67) nm in length and 172 ($\pm$ 55) nm in thickness. Their number varied from zero to four per stack. They had unique features in distinct cisternae: in *cis* cisternae, distensions were spherical or ovoid, and their lumen showed a loose filamentous pattern with little evidence of the aggregated form; in medial cisternae, they were more cylindrical and exhibited a structured pattern with more densely packed parallel threads; in *trans* cisternae, the packing was comparatively more dense. Figure 1A shows an example of a stack with at least four distensions exhibiting increasing packing density, presumably in the *cis-trans* direction. The $>$300 nm long body with striations perpendicular to its long axis is an immature secretory granule. Granules are known to mediate the transport of PC to the plasma membrane (Trelstad and Hayashi, 1979; Leblond, 1989). An example of a stack with one distension, a more common observation, is shown in Figure 1B.

The distribution of PC along the secretory pathway was examined with two monoclonal antibodies (MAbs): the first [hCL(I)] recognizes only the helical portion of PC (Ohtani et al., 1992) and therefore only binds to the protein in the folded state; the second (SP1.D8) is directed against the N-terminal propeptide and recognizes both the folded and the unfolded forms of PC (Foellmer et al., 1983). Figure 1C shows that distensions were intensely labeled by hCL(I). All the distensions were labeled by this antibody. No PC labeling was observed outside the distensions, namely in the flat regions of the Golgi cisternae. This indicates that all PC helices in the Golgi are assembled into aggregates in the distensions. The only other cellular structures labeled by hCL(I) were VTCs located very close to, or in continuity with, the ER (see Figures 5G–5K). Thus, the great majority of the immunoreactive folded PC was in Golgi distensions. The other antibody (SP1.D8) confirmed the labeling pattern obtained with hCL(I) and, in addition to Golgi distensions and VTCs, recognized numerous regions of the ER presumably containing unfolded PC being processed for export (Figure 1D).

As mentioned above, one of the objections to the maturation model is that cisternae containing supramolecular complexes might be part of an extended TGN rather than medial and *trans*-Golgi compartments (Farquhar and Palade, 1981; Becker et al., 1995). In the

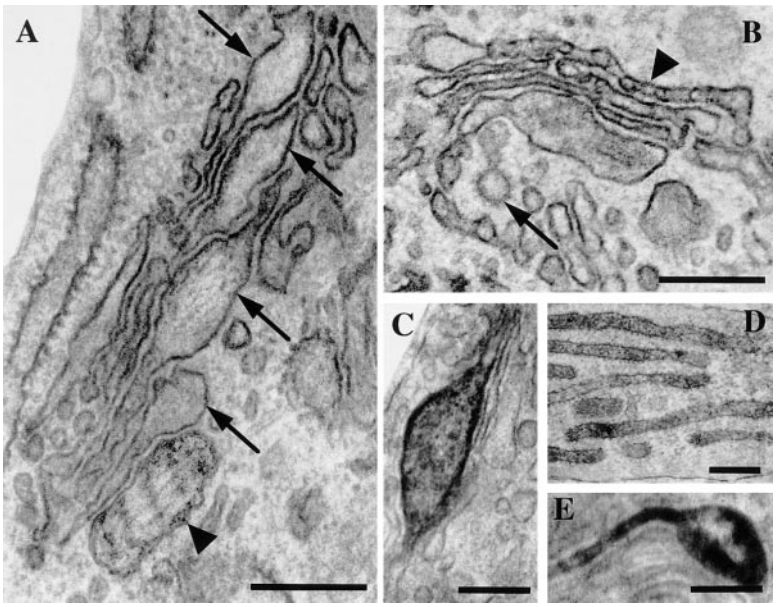

Figure 1. Ultrastructure and Localization of PC in the Golgi Complex

(A) A stack containing four distensions (arrows) to demonstrate the gradient in organization and packing density of PC filaments between the two poles of the stack. The arrowhead indicates a secretory granule (see Leblond, 1989).

(B) A stack containing one distension in a *trans* cisterna. Note the clathrin bud (arrow) and the perforated cisterna (arrowhead), marking the *trans* and the *cis*-Golgi poles, respectively.

(C) Distension immunolabeled for PC by the hCL(I) MAb.

(D) Areas of the ER are immunolabeled for PC by the SP1.D8 MAb.

(E) Distension in a cisterna immunolabeled for manII. Note that both the distension and the flat portion of the cisterna are labeled. Bars, 200 nm.

case of PC-secreting cells, however, the presence of distensions at all levels of the Golgi stacks has been established unequivocally (see Trelstad and Hayashi, 1979; Leblond, 1989) and is confirmed in Figures 1, 2, and 5. Nevertheless, to further address this concern, we determined whether some of the aggregate-including distensions contain mannosidase II (manII), a well-characterized medial Golgi enzyme (Rabouille et al., 1995). This experiment was carried out in rat tendon fibroblasts because the available anti-manII antibodies do not recognize the avian protein. The Golgi complexes of rat and chick tendon fibroblasts are very similar; in particular, the frequency and distribution of the aggregates were nearly indistinguishable between the two species (not shown). Figure 1E shows that an antibody against manII intensely labeled some of the distensions, in addition to the flat portions, of some cisternae. Thus, it is clear that PC aggregates reside not only in the TGN, but also in earlier Golgi compartments.

PC Aggregates Are Transported across the Golgi Stacks

To rule out the possibility that PC aggregates in Golgi distensions are stationary agglomerates of this protein, and to measure the intra-Golgi transit rate of the aggregates, we sought to synchronize the exit of PC from the ER and then visualize the movement of the aggregates across the stacks. As mentioned above, this can be achieved by exploiting the fact that PC folding in the ER requires proline hydroxylation. The prolyl hydroxylase can be selectively and reversibly inhibited by a class of iron chelators whose prototype is 2, 2′-dipyridyl (DPD); moreover, the folding inhibition is potentiated by removing the enzyme cofactor ascorbate (Harwood et al., 1976). We have used two DPD-based protocols. The first was simply to inhibit PC folding (and hence PC export from the ER) and visualize the behavior of the PC aggregates already present in the Golgi stacks. If the arrival of new PC from the ER is blocked, and if PC aggregates move anterogradely through the Golgi stacks, the aggregates should disappear first from *cis* cisternae and subsequently from medial and *trans* cisternae, with a time course reflecting their rate of transport across the Golgi stacks. This should generate the impression of a secretory wave leaving the organelle ("exiting wave"). The second protocol was to first inhibit PC folding for a period sufficient to accumulate the protein in the ER and empty the Golgi complex of aggregates, then release the folding block and, as the large amount of PC trapped in the ER gets folded and exported, observe PC aggregates as they reappear first in the *cis* and then in the more distal Golgi cisternae ("incoming wave" protocol).

An important requirement of this assay is that the polarity of Golgi stacks must be determined in order to assess the direction of this progression of aggregates. This was achieved in two ways. The routine approach was to use structural criteria, such as the presence of clathrin buds on the *trans* side of the Golgi stacks (see Experimental Procedures). This required the use of serial sectioning, since the polarity-defining features were often absent in individual sections of a stack. In such cases, consecutive images were analyzed in serial sections until the polarity-defining features were found and the orientation of the stack could be established (an example is shown in Figures 5A–5F). Stacks whose polarity could not be assessed unambiguously ($<$20%) were excluded from the experiment. An additional advantage of the serial sectioning approach was that the position of each PC aggregate (peripheral or central) in the cisterna could be determined. The second approach was to use ultrathin cryosections double immunogold labeled for PC and clathrin, a reliable *trans*-Golgi marker. In addition, the improved section-retrieval method in cryosectioning (Liou et al., 1996) allowed the visualization of COP coats at the *cis* side of the Golgi (Figure 3B, arrowheads).

The behavior of PC in DPD-treated ET fibroblasts was examined first by immunofluorescence (Figures 2a–2f).

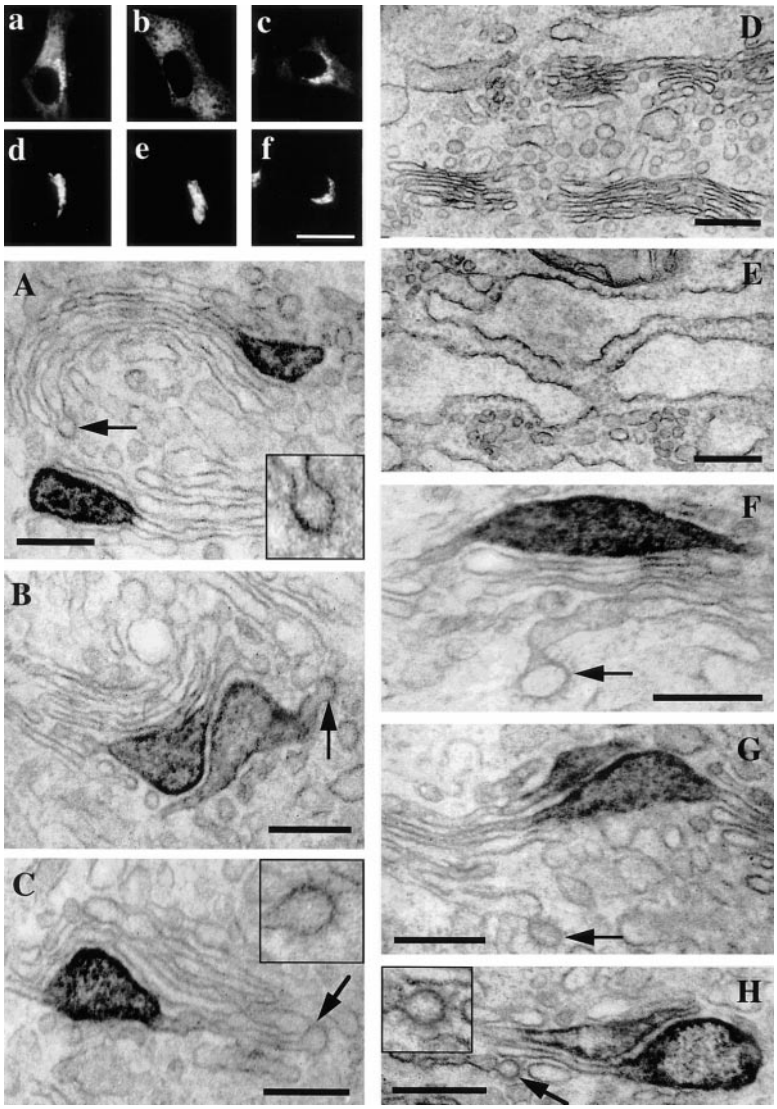

Figure 2. Use of DPD to Visualize the Transport of PC Aggregates through the Golgi Stacks

(a–f) Effects of DPD on the distribution of PC in an immunofluorescence experiment. ET fibroblasts were double-labeled for PC (by the LF68 antibody) (a–c) and for giantin (d–f). In control cells (a), PC was present both in the Golgi (by colocalization with giantin (d) and in the ER (by colocalization with calreticulin, not shown). After treatment with DPD for 60 min (b), PC was absent in the Golgi and abundant in the ER. When DPD was removed and cells were left to recover for 60 min (c), PC was concentrated again in the Golgi complex. Bar, 3.5 μm.

(A–E) Visualization of PC transport by immunoelectron microscopy using the "exiting wave" protocol. ET fibroblasts were treated with DPD for different times, fixed, and labeled. The polarity of the stacks was established by the presence of clathrin-coated buds (arrows) in the *trans* Golgi. The insets show magnifications of these clathrin buds. (A) Cells before exposure to DPD. Most stacks contained one or two distensions. The distensions could be present at all levels of the stacks. The micrograph shown here shows a stack with two distensions, in *cis* and medial cisternae. (B) After 10 min of DPD treatment, PC-containing distensions disappeared from *cis* cisternae but remained visible in *trans* and medial cisternae. (C) After 30 min of DPD treatment, PC-containing distensions were present only in *trans* cisternae. (D) After 60 min of DPD treatment, no distensions were visible and (E) the ER was greatly distended. Bars, 200 nm.

(F–H) The "incoming wave" protocol. ET fibroblasts were treated with DPD for 60 min. DPD was then washed out and cells were fixed at different times after washout. (F) Cells 10 min after DPD washout; PC-containing distension were found only in the *cis* cisterna. (G) Cells 20 min after DPD washout; distensions were in *cis* and medial cisternae. (H) Cells 40 min after DPD washout; distensions were in all cisternae (the stack shown here contains distensions in medial and *trans* cisternae). Bars, 200 nm.

After 60 min of treatment with DPD in the absence of ascorbic acid, PC disappeared from the Golgi and markedly increased in the ER. This is consistent with the notion that DPD blocks the exit of PC from the ER, while secretion of PC from the Golgi continues. When DPD was washed out, PC reappeared in the Golgi, indicating that the effect of DPD is reversible and the PC trapped in the ER can fold, exit, and reach the Golgi. The traffic of PC aggregates across the stacks was next followed by electron microscopy (Figures 2A–2H). Cells were stained either by tannic acid or immunolabeled by the HRP technique. Figures 2A–2E show the results of the "exiting wave" experiment. DPD caused a gradual but profound reduction in the number of PC-containing distensions from the Golgi complex in about 40 min. This loss was first evident in *cis*-, then medial, and finally in the *trans*-Golgi cisternae. This is indeed the expected sequence of events if aggregates move through the Golgi stacks in the *cis*-*trans* direction. A morphometric quantitation of these observations is shown in Figure 4A. There were on average 24 PC aggregates in the Golgi of each control cell, distributed roughly uniformly among the Golgi cisternae. Aggregates were reduced in DPD-treated cells with a $t_{1/2}$ of 13 min in *cis* and 32 min in *trans* cisternae. Thus, the transit time of PC aggregates across the Golgi stacks, calculated from the difference between the two $t_{1/2}$ values, is 19 min. Importantly, aggregates located near the center of the cisternae disappeared at the same rate as those near the cisternal rims. An additional important observation was that the size of the PC-containing distensions was not affected by the DPD treatment. At all times during the treatment, the thickness of the remaining distensions remained the same as in control cells (190 $\pm$ 50 nm). This is of interest because it indicates that aggregates move en-bloc, rather than by disassembly and forward transport of

individual PC helices (see Discussion). Moreover, as in control cells, PC was never found in the flat portions of the Golgi cisternae (namely, it was never found outside the distensions), further supporting the idea that PC aggregates do not disassemble or release individual PC helices, since helices would probably be able to diffuse into the flat domains of the cisternae. Concomitant with the disappearance of PC aggregates from the Golgi, the ER became swollen due to the accumulation of unfolded PC (Figure 2E). The cells, however, remained viable and showed no signs of general toxicity for up to 1 hr in DPD.

In the complementary approach ("incoming wave"), ET fibroblasts were treated with DPD for 60 min. This incubation time is sufficient to empty the Golgi complex of PC and load the ER with the unfolded protein (see Figures 2D and 2E). DPD was then washed away, ascorbic acid added to the cells to facilitate PC refolding, and the reappearance of PC aggregates in the Golgi followed by electron microscopy. Folded PC reappeared first in VTCs. VTCs did not label for PC immediately, but 5 min after DPD washout, they exhibited staining of their central tubular parts (not shown). By contrast, the surrounding round profiles (identifiable as vesicles in serial sections) remained unlabeled. Thus, these VTCs were very similar to those seen in untreated cells. By 10 min after DPD washout, cisternal distensions containing PC were detected in the *cis*-Golgi cisternae and then, successively, in the medial and trans cisternae (Figures 2F–2H). This is consistent with the progression of the newly formed aggregates through the Golgi stacks in the *cis*-*trans* direction. A morphometric assessment of the time course of reappearance of PC aggregates at different levels of the Golgi stacks is shown in Figure 4B. The $t_{1/2}$ was 13 min for the *cis* cisternae and 35 min for the *trans* cisternae. This time course is very similar to the time of clearance of PC in the "exiting wave" experiments. The intra-Golgi transit time of PC aggregates, calculated as the difference between the $t_{1/2}$ values of PC reappearance in the *cis* and the *trans* cisternae, was 22 min (again, similar to the value found using the "exiting wave" protocol). Interestingly, by 60 min after DPD washout, the number of PC aggregates in the Golgi was 42% higher than in the control cells (Figure 4B). This should be due to PC overload in the ER during the folding block, resulting in a higher than normal input of this protein into the Golgi once the block is released.

The "incoming wave" experiment was then repeated using the cryoimmunogold labeling approach. PC was labeled with the SP1.D8 antibody, and Golgi polarity was determined by labeling the *trans* end of the stacks with an anti-clathrin antibody. As expected, after 60 min of DPD-induced block, the ER was heavily labeled for PC (Figure 3A). Most Golgi stacks were depleted of label (not shown). When the block was released for 15 min, PC-containing distensions appeared in *cis* but not *trans* cisternae (Figure 3B). A semiquantitative analysis (Table 1) showed that 88% of the labeling occurred on the *cis* side of the stack. Sixty minutes after DPD washout, the ER was almost devoid of PC (Figure 3C). Moreover, PC aggregates had repopulated all the levels of the stack and were most numerous in the *trans* cisternae (Figures 3D–3F and Table 1). Occasionally, distensions contained clathrin-coated membranes (Figure 3E, inset). Mature and immature secretory granules were also visible (Figure 3F). These data are in excellent agreement with the results of the immunoperoxidase experiments in Figure 2.

Finally, we examined whether DPD might have global effects on protein traffic. The ts045 viral protein VSV-G was employed as a traffic marker (Bergmann, 1989). This mutant protein accumulates in the ER at 40°C but rapidly moves to the Golgi upon shifting the temperature to 32°C. The $t_{1/2}$ for acquisition of endoH resistance by the VSV-G protein was used as an index of transport of the protein to the medial Golgi (Bergmann, 1989). This $t_{1/2}$ was found to be 15 min ($\pm$ 2) in control cells, 16 min ($\pm$ 5.5) in the presence of DPD applied simultaneously with the temperature shift to 32°C ("exiting wave" protocol), and 15 min ($\pm$ 4) in cells exposed to DPD for 1 hr and washed free of this agent just before the temperature shift ("incoming wave" protocol). Thus, DPD does not affect the general traffic machinery. This agrees with previous evidence that DPD does not affect the secretion of laminin (Kim and Peterkofsky, 1997). Therefore, the rates of intra-Golgi transport of PC as measured here reflect the physiological PC transport.

In conclusion, these findings demonstrate that PC aggregates move across the Golgi in the *cis*-*trans* direction and that the PC intra-Golgi transport takes approximately 20 min.

The Transport of PC Aggregates along the Secretory Pathway Accounts for PC Secretion

To determine whether the movement of PC aggregates along the secretory pathway accounts for the rate of PC secretion, we used the "exiting wave" and the "incoming wave" DPD-based protocols in experiments of PC release. In the first protocol, cells were treated with DPD, and the time course of PC release was examined. The rationale of this experiment is that if the progression of PC aggregates is the main means of PC transport, PC release should continue for some time after the DPD-mediated folding block. In fact, it should continue precisely for the time required for the aggregates present in the Golgi prior to the block to pass through the secretory pathway and be secreted. After this time, PC release should fall to low levels, concomitant with the disappearance of the aggregates. The time lag before secretion is inhibited can be calculated: as shown earlier (Figure 4A), PC aggregates begin to disappear from the *trans* cisternae approximately 25 min after the folding inhibition. In addition, the transport time of PC from the TGN to the plasma membrane is approximately 5 min, as indicated by experiments of PC release after accumulation of the protein in the TGN at 20°C (not shown). Therefore, PC release should begin to fall approximately 30 min after the application of DPD. Figure 4C shows that, indeed, PC release proceeded nearly unperturbed for 30 min after the DPD-induced folding block and then gradually decreased to a low plateau.

The complementary "incoming wave" experiment is shown in Figure 4D. Unfolded PC was accumulated in the ER for 60 min in the presence of DPD, and then the folding block was removed. According to the logic just

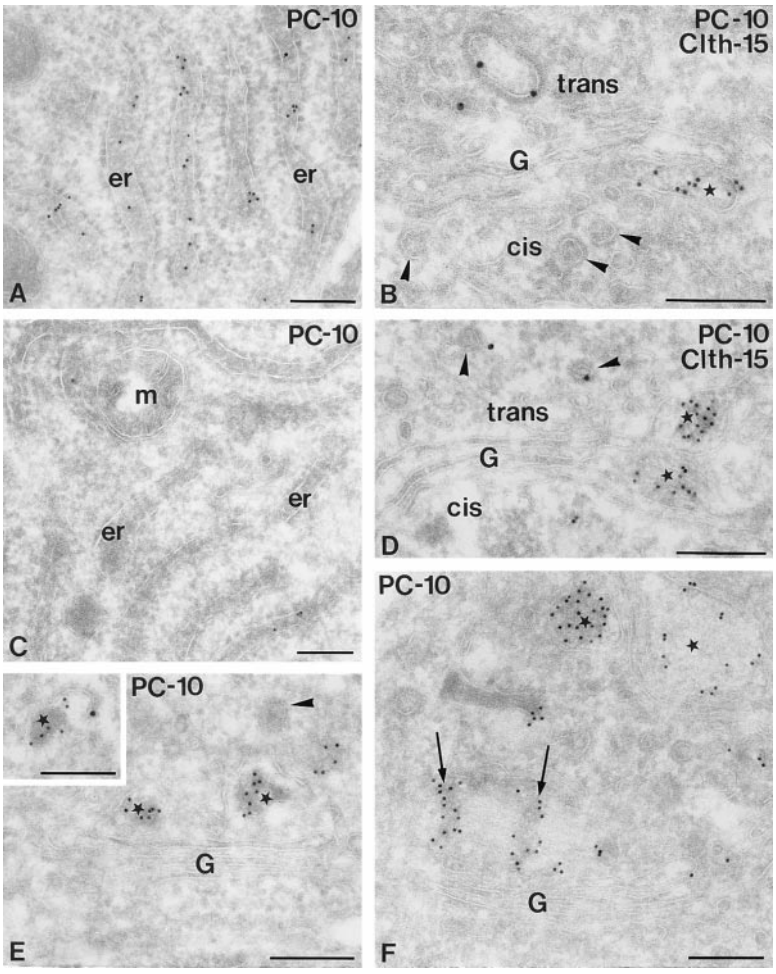

Figure 3. Localization of PC in the Golgi Stacks by Immunogold Labeling

Ultrathin cryosections of ET fibroblasts were single immunolabeled for PC with 10 nm gold (A, C, E, and F) and double immunolabeled for PC with 10 nm gold and for clathrin (Clth) with 15 nm gold (B, D, and inset in E), as indicated in the figure.

(A) Exposure to DPD for 60 min. The endoplasmic reticulum (er) is heavily labeled for PC.

(B) Fifteen minutes after DPD washout. A distension (asterisk) containing PC is present in a *cis*-Golgi cisterna. Note the characteristic COP coats (arrowheads) on membranes at the *cis*-Golgi side, which are thinner than the clathrin coat present on a *trans*-Golgi vesicle. G, Golgi stack.

(C–F) Sixty minutes after DPD washout. (C) PC labeling in the ER is scarce. m, mitochondrion. (D) PC-containing distensions (asterisks) are observed at different levels of the Golgi stack (G). The flattened parts of the Golgi cisternae do not label for PC. Arrowheads point to clathrin-coated vesicles at the *trans*-Golgi side. (E) Distensions or immature secretory granules (asterisks) at the *trans*-Golgi side exhibiting PC labeling over their electron-dense cores. Note the fuzzy coated bud (arrowhead) on a distension. G, Golgi stack. The inset shows the clathrin labeling of a similar coat. (F) Secretory granules and immature secretory granules (asterisks) containing fibrous material. The labeling for PC is restricted to the edge of the fibers within electron-dense areas (arrows). G, Golgi stack. Bars, 200 nm.

described for the "exiting wave" experiment, PC secretion should remain low or undetectable for about 30 min, the time needed for PC aggregates to traverse the secretory pathway (see Figure 4B). Then it should increase rapidly. Figure 4D shows that PC release, indeed, resumed 30 min after the removal of DPD. Moreover, 45 min after DPD washout, the PC release rate became higher than in control cells, presumably reflecting the fact that the large amounts of protein accumulated in the ER during the DPD-induced block must now be discharged. This is in excellent agreement with the morphometric measurements of the number of PC aggregates in Golgi stacks (see Figure 4B). Altogether, these data provide strong evidence that the intracellular transport of PC aggregates is the sole mechanism for PC transport and secretion.

PC Does Not Leave the Lumen of Golgi Cisternae during Intra-Golgi Transport

The next obvious question is whether PC aggregates are transported across the Golgi stacks in dissociative carriers or move through this organelle without leaving the lumen of the Golgi cisternae. The classical transport carriers (i.e., COPI 60–90 nm vesicles) can be ruled out because of the shape and length of the PC helix. This leaves the following alternatives. One, entire aggregate-containing distensions detach from donor cisternae and fuse with the successive cisterna in the stack. If this occurred, there should be free unattached distensions in the act of moving from one cisterna to another. Additionally, the free distensions should arise through the protrusion of the aggregate and the formation of membranous necks connecting distension and cisterna. This neck should then undergo fission, thus releasing the distended membrane containing the PC aggregate. Two, aggregates disassemble into smaller units (PC helices). The units are incorporated into elongated transport carriers (at least 300–400 nm long). These carriers then fuse with the successive cisterna, where the PC helices reassemble into aggregated forms.

To test these two hypothetical schemes, we carried

Table 1. Distribution of PC in the Golgi Cisternae after Release of the DPD-Induced Block

Time	G1	G2	G3	G4
15 Min	62 ± 7.7	26 ± 8.2	10 ± 4.3	2 ± 1.7
60 Min	18 ± 3.6	15 ± 5.8	36 ± 9.3	31 ± 7.8

Numbers represent the percent (mean + SE) of the gold particles labeling for PC counted over Golgi stacks in cryosections. The quantitation was done in 20 random Golgi stacks (per time point) at 15 and 60 min after DPD washout. The experiment was carried out using the "incoming wave" protocol (see text). Golgi cisternae are numbered from G1 (*cis*-most) to G4 (*trans*-most).

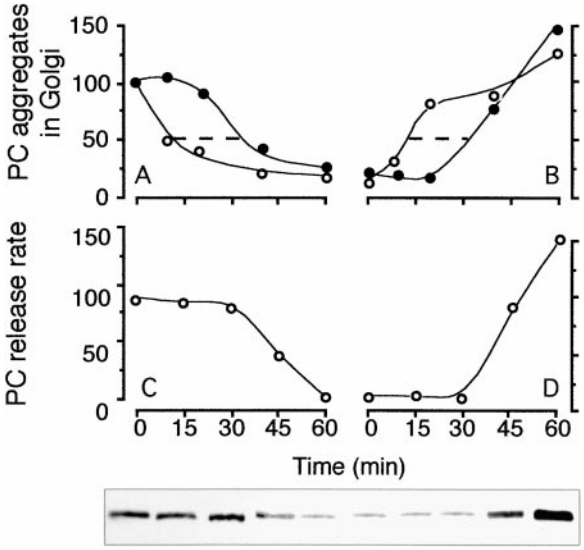

Figure 4. The Transport of PC Aggregates Accounts for PC Release

(A and B) Morphometric quantitation of "exiting wave" and "incoming wave" experiments. The location of distensions was determined as described in Experimental Procedures. Only distensions in *cis* or in *trans* cisternae were included in the experiment. (A) Time course of the DPD-induced reduction in the number of PC-containing distensions in *cis* (empty circles) and *trans* (filled circles) cisternae. DPD (0.3 mM) was applied at time 0, and the cells were fixed at the times indicated in the Figure. (B) Time-dependent increase of PC-containing distensions after removal of DPD. Cells were treated with DPD (0.3 mM) for 60 min. DPD was then washed out (time 0) and the cells were fixed at the times indicated in the figure. Greater than 60 distensions were analyzed per time point, in three different experiments. The S. E. never exceeded 10% of the mean.

(C and D) Biochemical quantitation of PC release during "exiting wave" and "incoming wave" experiments. (C) Inhibitory effect of DPD on the release of PC. DPD (0.3 mM) was applied at time 0 in fresh medium. The extracellular medium was removed at the indicated times and fresh medium was layered on the cells, kept for 5 min, collected for analysis of PC (see Experimental Procedure), and replaced again with fresh medium. (D) Recovery of the PC release rate after DPD washout. Cells were treated with DPD (0.3 mM) for 60 min. DPD was then washed out (time 0), and the PC secreted in the medium after washout was measured at the times indicated in the figure. Data are means of four determinations. Similar results were obtained in four different experiments. SD never exceeded 15% of the means. The bottom panel shows representative samples of PC released in the extracellular medium, collected at the specified time points, separated by SDS-PAGE, and detected by Western blotting.

out three-dimensional reconstructions of Golgi stacks based on consecutive serial sectioning of a large number of both routinely stained and immunolabeled cells. The horseradish peroxidase (HRP)-based technique was used for immunodetection of PC (Brown and Farquhar, 1989) because the HRP-labeled samples are suitable for serial sectioning and the stain clearly delineates the profile of the antigen-containing membranes. This greatly facilitates the recognition/reconstruction of PC-containing structures in consecutive sections. The labeling conditions were checked and shown to be optimal for intralumenal antigens in cisternae, VTCs, and Golgi vesicles using different antigens and cell lines (see Experimental Procedures).

The majority of the PC aggregates (70%) were located near the rims of cisternae but did not protrude from the cisterna. Twenty-eight percent of the aggregates were located in the cisternal core. A minor fraction (2%) of the aggregates protruded moderately from the rims of cisternae. Images suggesting budding/fission of a PC aggregate (for instance, an aggregate protruding by the majority of its length, a narrowing neck between a cisterna and a protruding aggregate, or an aggregate disconnected from the cisternae) were not found in greater than 600 distensions observed. All aggregates were always clearly embedded within cisternae. Figures 5A–5F show an example of serial sections of a PC aggregate–containing cisterna. Figures 6A and 6B show the three-dimensional reconstruction of the same cisterna based on manual tracing of the cisternal contours.

The second type of hypothetical Golgi transport carriers are >300 nm long tubules. They should be relatively straight, adjacent to Golgi stacks, and should contain PC helices. In addition, there should be elongated buds with similar characteristics. We define these structures as Golgi transport tubules. They were searched for first in cells immunolabeled for PC, using the same samples in which VTCs exhibited intense staining for PC (see below). Neither PC-labeled free tubules in the vicinity of the Golgi complex, nor long tubular buds emanating from cisternae were observed, in spite of the fact that 30 complete Golgi complexes were analyzed by serial sectioning. Golgi transport tubules were also searched in both rapidly fixed osmium-stained and cryofixed cells (our unpublished results). Although in areas between adjacent stacks a convoluted tubular-saccular meshwork was present (the noncompact zone, see Rambourg and Clermont, 1990), no relatively straight, long tubular structures were seen to lie close to, or emanate from, Golgi distensions. In contrast, normal, roundish, presumably COPI- or clathrin-coated buds and vesicles were frequently seen on or near cisternal rims. However, these vesicles never labeled for PC.

The only structures that did not belong to a stack but labeled for PC were VTCs. They were easily recognized by their close association with the ER, as well as by the characteristic presence of a tubule/saccule closely adjacent to a cluster of vesicles (Bannykh et al., 1996). In order to define the structure of PC-containing VTCs, we used serial sectioning. An example is shown in Figures 5G–5K. The PC-containing VTC appeared as elongated structures with a tubular-saccular portion of >70–100 nm in diameter, >300 nm in length, adjacent to the ER and surrounded by 60–90 nm vesicles. In general, the tubular portions of VTCs were strongly labeled for PC. Most of the vesicular profiles, instead, were not labeled. The few that were labeled, moreover, usually appeared to represent cross sections of tubules (for instance, compare Figures 5J and 5K). Whether this is always the case, however, remains to be clarified (see Discussion). The total number of PC-containing VTCs was about 30 per cell.

Discussion

The Secretion of PC Is Mediated by the Transport of PC Aggregates through the Golgi Stacks

The only compelling interpretation of the experiments of synchronization of PC export from the ER is that, when

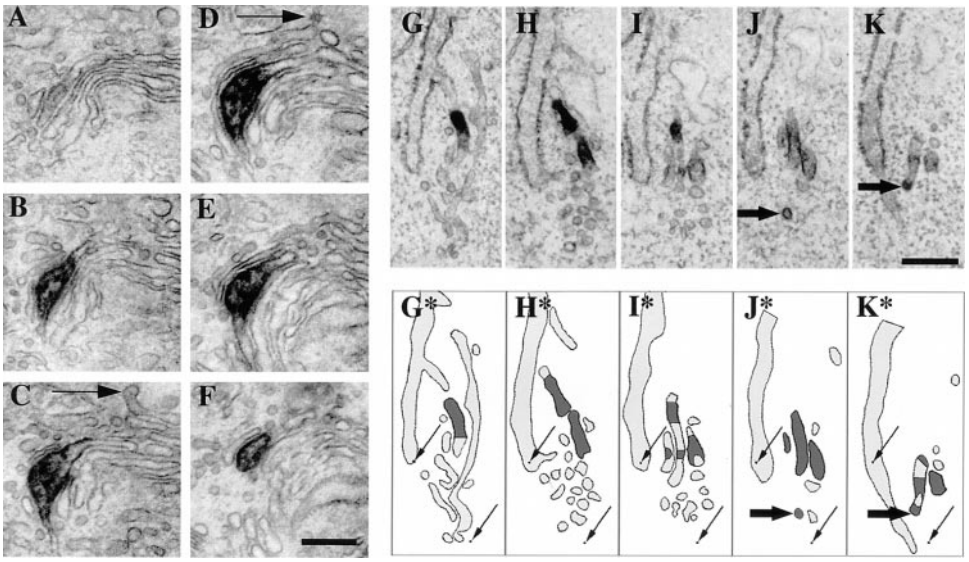

Figure 5. PC-Containing Distensions and VTCs in Consecutive Serial Sections

(A–F) A PC-containing distension in six consecutive serial sections. A clathrin-coated bud (arrow) labels the *trans* side of the stack.

(G–K) A VTC labeled for PC in five consecutive serial sections (the central part of a series of ten images). The VTC contains a central tubule-like part heavily labeled for PC, which emerges from the rough ER, decorated by ribosomes. In (J), (K), (J*), and (K*), arrows indicate what is seemingly an isolated stained vesicle in (J) but turns out to be part of the PC-containing tubule in the next section (K). More peripheral roundish or elongated and sometimes convoluted narrow profiles do not label for PC.

(G*–K*) Manually traced contours of the VTC and the other structures shown in the adjacent panels. The fiducial marks for superimposition of the sections are indicated by thin arrows. The presence of the immunolabel for PC is indicated by the dark areas. Bars, 200 nm.

PC folding is blocked, aggregates in the *cis* cisternae disappear first because they pass into medial compartments and are no longer replaced by a new load of PC from the ER. Medial aggregates disappear next because they move to *trans* cisternae without being replaced by *cis* material ("exiting wave"). When the block is removed, PC that was accumulated in the ER rapidly folds, exits the ER, organizes into aggregates, and resumes its travel through the Golgi stacks, moving from one level in the stack to the next ("incoming wave"). Thus, PC aggregates move in the anterograde direction. Moreover, the transport of PC aggregates through the secretory pathway is the sole or main mechanism of PC intracellular traffic and secretion, as indicated by the following lines of evidence. First, the secretion of PC and the intracellular movement of the aggregates were tightly coupled in time. Second, all of the folded PC in the Golgi was located in the aggregates, both at steady state and during exiting and incoming wave experiments. Third, the rate of PC intracellular transport in ET fibroblasts, as assessed by others by pulsing PC with radioactive proline and following it along the secretory pathway (Harwood et al., 1976; Kao et al., 1977), is in agreement with our measurements.

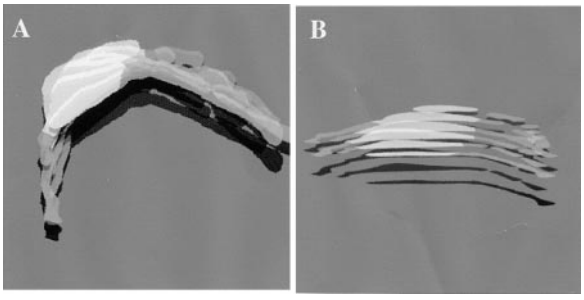

Figure 6. Three-Dimensional Reconstructions of a PC-Containing Cisterna

Serial sections of the distension in Figures 5A–5F were digitized and used for the reconstruction, using the InSIGHT-IQ1.1 Meridian software. (A) and (B) represent the same object seen from different points of view. The PC aggregate (light grey) is clearly embedded in the cisterna (dark grey).

PC Does Not Exit the Lumen of Cisternae during Intra-Golgi Transport

How are PC aggregates transported across Golgi stacks? The physical properties and dimensions of PC helices and the association of helices in aggregates place constraints on the shape and size of hypothetical PC carriers. Because of its length and rigidity, transport of PC is incompatible with traffic via 60–90 nm transport vesicles. However, as mentioned above, there could be alternative carriers for PC traffic. The properties of PC indicate that such carriers could be of two types. They could be distensions containing entire aggregates that detach en-bloc from the cisterna ("transport vacuoles") or they could be "transport tubules," containing individual PC helices traveling from the aggregate in one cisterna to the successive cisterna in the stack. The first possibility is excluded because aggregates are always embedded in the cisternae. Thus, the structure itself of the aggregate-containing distensions is clearly incompatible with the possibility of transport vacuoles. Moreover, the observation that the numerous aggregates located near the center of the cisternae move through the

Golgi at the same rate as peripheral ones makes such a possibility even more implausible. The other hypothetical carrier, the transport tubule, is excluded based on two independent lines of evidence. First, Golgi transport tubules were never observed; however, 30 tubular portions of VTCs immunolabeled for PC were found per cell. It is therefore very unlikely that Golgi transport tubules, if they are transport intermediates, should not be detected, especially considering that such tubules should transport across each pair of successive cisternae the same amount of cargo that is transferred from the ER to the Golgi by the VTCs. This becomes even more unlikely considering that 30 complete Golgi complexes were analyzed by serial sectioning in our search for transport tubules. In contrast, roundish buds and vesicles were a common observation, but they never labeled for PC. Second, if tubules containing PC helices functioned as carriers, it should be assumed that helices disassemble from aggregates in a cisterna and move, one by one, to the successive cisterna. This mechanism predicts that, in the presence of a folding block, if helices move out of a given aggregate without being replaced from the proximal cisterna, the size of the aggregate should gradually decrease. However, this was not the case: the block of PC folding and export from the ER caused a reduction in the number of aggregates in a *cis-trans* sequence but not in their size, which remained remarkably constant throughout the process of exit of these structures from the Golgi complex. Such constancy in size can easily be explained by the cisternal maturation mechanism. Furthermore, the observation that immunoreactive folded and unfolded PC was never detected in Golgi cisternae outside aggregates indicates that PC aggregates are stable and unlikely to dissociate into monomers at the rate required for this disassembly-reassembly mode of transport.

Conclusions

Collectively, our findings show that PC is secreted by moving along the Golgi stacks without leaving the lumen of the cisternae. This is a central feature of the cisternal maturation-progression model. Whether other viable traffic models exist that might accommodate this feature seems very unlikely but cannot be completely excluded at this time (e.g., traffic by "bolus"; see Ayala, 1994). Based on our results, we propose that the intracellular traffic of PC occurs as follows: PC helices move from the ER toward the Golgi complex inside the tubular portion of VTCs. There, they fuse with each other and form a new *cis*-Golgi cisterna. The process of PC aggregation begins in this compartment. The *cis* cisterna then apparently progresses through the stack by going through successive maturation stages during which the aggregates can be imagined as passive objects lying inside the lumen while the cisternal membrane flows around them in the retrograde direction (Mironov et al., 1997). Meanwhile, the lumenal environment gradually changes, causing the increasing condensation of the aggregates and resulting in the formation of secretory granules ready for secretion.

A question emerging from these findings concerns the ER–Golgi transport step. PC monomers are believed to fold in the ER (Beck et al., 1996), yet they are too long to enter the COPII-coated vesicles involved in export from this organelle. A possibility is that PC might exit the ER inside tubules elongating directly from the ER surface. As has been previously noted, carrier structures might have sufficient flexibility in their forming machinery to adapt to unusually large cargoes (Schekman and Mellman, 1997). Alternatively, PC might be exported from the ER via conventional transport vesicles. However, to fit into such vesicles, PC should be in a partially unfolded state. This dilemma remains to be resolved in further studies.

Finally, while our data implicate the cisternal maturation mechanism in the transport of supramolecular aggregates, they also raise the possibility that such a mechanism might play a role in all cell types. The observation of Presley et al. (1997) that VTCs move en bloc to the Golgi complex is in line with this notion. Additional approaches will be required in the future to test the generality of the maturational mode of traffic. A strong possibility is that cisternal maturation may coexist with other intra-Golgi traffic mechanisms, such as anterograde carrier vesicles (see Rothman and Wieland, 1996). In any case, the molecular mechanisms of cisternal maturation, primarily those sustaining the retrograde transport of Golgi enzymes, should now be worked out.

Experimental Procedures

Cells and Reagents

Tendon fibroblasts from 15-day-old chicken embryos or from tails of newborn rats were isolated as described previously (Colombatti et al., 1987). The cell suspension was then gently centrifuged, and the cells were resuspended in complete DMEM containing 1% adult bovine serum, plated into Petri dishes or 8-well glass chamber slides (Nunc, Roskilde, Denmark) previously coated with 30 μg/ml fibronectin, and kept for 18 hr at 90% confluence before the experiments.

All reagents were obtained from sources described earlier (Buccione et al., 1996) unless otherwise noted. The monoclonal antibody against the N-terminal peptide of the α1 chain of PC I (SP1.D8) was from the Developmental Studies Hybridoma Bank, University of Iowa (Iowa City); the monoclonal antibody against the helical portion of collagen I [hCL(I)] was from Fuji Chemical Industries (Toyama, Japan); the polyclonal antibodies (LF42, LF68) against the C-terminal peptide of the α1 chain of PC were from L. W. Fisher (NIH, Bethesda); the polyclonal antibody against manII was from K. Moremen (University of Georgia, Athens); and the polyclonal antibody against clathrin was from S. Corvera (University of Massachussets). Ascorbic acid, human fibronectin, and collagenase I were obtained from Sigma (St. Louis), and 2, 2 dipyridyl was obtained from Acros Organics (New Jersey). Fab fragments conjugated with peroxidase were from Biosys (Compiegne, France).

Immunofluorescence, Electron Microscopy, Immunogold Labeling of Cryosections, Stereology, and 3D Reconstruction

ET fibroblasts grown in glass chamber slides were prepared for immunofluorescence, transmission electron microscopy, immunoperoxidase–electron microscopy, and immunogold labeling of cryosections exactly according to previously described protocols (Brown and Farquhar, 1989; Liou et al., 1996). Double immunogold labeling was done with 10 and 15 nm protein A/gold particles. The antibody dilutions for immunoperoxidase–electron microscopy were 1:50 for hCL(I), 1:25 for SP1.D8, and 1:500 for anti-manII. The immunoperoxidase–electron microscopy protocol was tested for efficiency of labeling. It afforded reliable staining of PC and manII in the Golgi complex of fibroblasts (see Results), of manII and VSV-G in Golgi cisternae, and of tubules and mitotic Golgi vesicles in both

NRK and RBL cells (our unpublished observations). The same protocol has been previously reported to efficiently label manII in Golgi cisternae and clathrin-coated buds (Velasco et al., 1993), as well as ERGIC 58 in *cis*-Golgi tubules and vesicles (Jantti et al., 1997).

Serial sections were prepared exactly as described by Bannykh et al. (1996). For three-dimensional reconstructions, serial images were recorded and the contours of structures of interest were manually traced and transformed into digitized form. VTCs were defined according to Bannykh et al. (1996). The digitized contours were then used for three-dimensional reconstructions using the InSIGHT-IQ1.1 (Meridian Instruments, Inc.).

In the "wave" experiments, the number and average size of PC-containing distensions in *cis*- and *trans*-Golgi cisternae were estimated using established morphometric procedures (the disector and fractionator method, Gundersen, 1986). The polarity of stacks was established either by clathrin immunogold labeling or by several structural criteria: the most important was the presence of identifiable clathrin buds on the *trans* side; accessory criteria were the presence of COP coats at the *cis* side of the Golgi stacks, the characteristic fenestrated appearance of the *cis* most Golgi element, the peeling-off configuration of the TGN elements (see Rambourg and Clermont, 1990), and the close vicinity of *trans* cisternae with easily identifiable PC secretory granules. If these features were absent in a given section, consecutive serial images were analyzed until the orientation of the stack could be defined.

Assays of PC Release

Cells were plated as for morphological experiments and treated as described in Results. At the end of the experiment, the incubation media were collected and proteins were precipitated with 10% trichloroacetic acid and analyzed by SDS-PAGE and immunoblotting, using the polyclonal anti-PC antibodies LF68 and LF42 and the monoclonal antibody SP1.D8 at 1:1000 dilutions. The LF68 and SP1.D8 antibodies were used for quantitation. In order to construct a calibration curve, increasing amounts of collagen were processed in parallel with the experimental samples. Immunostained bands of PC α1 (160 kDa) were analyzed by NIH Image Analysis Program. The amount of PC in the samples was calculated from the linear portion of the collagen calibration curve.

Acknowledgments

We thank V. Malhotra (University of California, San Diego) for many fruitful discussions and C. P. Berrie for critical editorial work on the manuscript. J. M. Griffith is acknowledged for her excellent assistance in immunogold labeling experiments. We thank J. Smith (NASA Ames Research Center, CA) for the 3D reconstruction using the ROSS software; H. P. Bachinger (Shriners Hospital, Portland) for discussions on the structure of procollagen; K. Moremen (University of Georgia, Athens) for the gift of the polyclonal anti-manII antibody; L. W. Fisher (NIH, Bethesda, Maryland) for the polyclonal anti-PC antibodies LF68 and LF42; H. P. Hauri (University of Basel, Basel, Switzerland) for the monoclonal anti-giantin antibody; and A. Colombatti (Aviano, Italy) for help in setting up the ET fibroblast model system. The antibody SP1.D8 developed by Dr. H. Furthmayr was from Hybridoma Bank, University of Iowa, Department of Biological Science. This research was supported by the Italian National Research Council (Convenzione C. N. R.-Consorzio Mario Negri Sud), the Italian Association for Cancer Research (AIRC), the Italian Foundation for Cancer Research (FIRC), and Telethon Italia. L. B. was the recipient of a fellowship from the Centro di Formazione e Studi per il Mezzogiorno, and J. A. M.-M was the recipient of a M. Curie fellowship from the ER (TMR programme, ERBFMBICT 961446).

Received June 22, 1998; revised November 10, 1998.

References

Ayala, J.S. (1994). Transport and internal organization of membranes: vesicles, membranes networks and GTP-binding proteins. J. Cell Sci. *107*, 753–763.

Bachinger, H.P., Morris, N.P., and Davis, J.M. (1993). Thermal stability and folding of the collagen triple helix and the effects of mutations in osteogenesis imperfecta on the triple helix of type I collagen. Am. J. Med. Genet. *45*, 152–162.

Bannykh, S.I., and Balch, W.E. (1997). Membrane dynamics at the endoplasmic reticulum-Golgi interface. J. Cell Biol. *138*, 1–4.

Bannykh, S.I., Rowe, T., and Balch, W.E. (1996). The organization of endoplasmic reticulum export complexes. J. Cell Biol. *135*, 19–35.

Beck, K., Boswell, B., Ridgway, C., and Bachinger, H.P. (1996). Triple helix formation of procollagen type I can occur at the rough endoplasmic reticulum membrane. J. Biol. Chem. *271*, 21566–21573.

Becker, B., Bolinger, B., and Melkonian, M. (1995). Anterograde transport of algal scales through the Golgi complex is not mediated by vesicles. Trends Cell Biol. *5*, 305–307.

Bergmann, J.E. (1989). Using temperature-sensitive mutants of VSV to study membrane protein biogenesis. Methods Cell Biol. *32*, 85–110.

Brodsky, B., and Ramshaw, J.A. (1997). The collagen triple-helix structure. Matrix Biol. *15*, 545–554.

Brown, W.J., and Farquhar, M.G. (1989). Immunoperoxidase methods for the localization of antigens in cultured cells and tissue sections by electron microscopy. Methods Cell Biol. *31*, 553–569.

Buccione, R., Bannykh, S., Santone, I., Baldassarre, M., Facchiano, F., Bozzi, Y., Di Tullio, G., Mironov, A., Luini, A., and De Matteis, M.A. (1996). Regulation of constitutive exocytic transport by membrane receptors. A biochemical and morphometric study. J. Biol. Chem. *271*, 3523–3533.

Colombatti, A., Bonaldo, P., Ainger, K., Bressan, G.M., and Volpin, D. (1987). Biosynthesis of chick type VI collagen. I. Intracellular assembly and molecular structure. J. Biol. Chem. *262*, 14454–14460.

Farquhar, M.G., and Palade, G.E. (1981). The Golgi apparatus (complex)-(1954–1981)-from artifact to center stage. J. Cell Biol. *91*, 77S–103S.

Foellmer, H.G., Kawahara, K., Madri, J.A., Furthmayr, H., Timple, R., and Tuderman, L. (1983). A monoclonal antibody specific for the amino terminal cleavage site of procollagen type I. Eur. J. Biochem. *134*, 183–189.

Gundersen, H.J.G. (1986). Stereology of arbitrary particles. J. Microsc. *143*, 3–45.

Harwood, R., Grant, M.E., and Jackson, D.S. (1976). The route of secretion of procollagen. Influence of $\alpha\alpha'$bipyridyl, colchicine and actinomicin A on the secretory process in embryonic-chick tendon and cartilage cells. Biochem. J. *156*, 81–90.

Jantti, J., Saraste, J., and Kuismanen, E. (1997). Protein segregation in peripheral 15 degrees C intermediates in response to caffeine treatment. Eur. J. Cell Biol. *74*, 150–164.

Kao, W.W., Berg, R., and Prockop, D.J. (1977). Kinetics for the secretion of procollagen by freshly isolated tendon cells. J. Biol. Chem. *23*, 8391–8397.

Kim, Y.-R., and Peterkofsky, B. (1997). Differential effects of ascorbic depletion and α,α'-dipyridyl treatment on the stability, but not on the secretion, of type IV collagen in differentiated F9 cells. J. Cell. Biochem. *67*, 338–352.

Leblond, C.P. (1989). Synthesis and secretion of collagen by cells of connective tissue, bone, and dentin. Anat. Rec. *224*, 123–138.

Liou, W., Geuze H.J., Slot, J.W. (1996) Improving structural integrity of cryosections for immunogold labeling. Histochem. Cell Biol. *106*, 41–58.

Mironov, A.A., Weidman, P., and Luini, A. (1997). Variations on the intracellular transport theme: maturing cisternae and trafficking tubules. J. Cell Biol. *138*, 481–484.

Ohtani, H., Kuroiwa, A., Obinata, M., Ooshima, A., and Nagura, H. (1992). Identification of type I collagen-producing cells in human gastrointestinal carcinomas by non-radioactive in situ hybridization and immunoelectron microscopy. J. Histochem. Cytochem. *40*, 1139–1146.

Pelham, H.R. (1998). Getting through the Golgi complex. Trends Cell Biol. *8*, 45–49.

Presley, J.F., Cole, N.B., Schroer, T.A., Hirschberg, K., Zaal, K.J.,

and Lippincott-Schwartz, J. (1997). ER-to-Golgi transport visualized in living cells. Nature *389*, 81–85.

Rabouille, C., Hui, N., Hunte, F., Kieckbusch, R., Berger, E.G., Warren, G., and Nilsson, T. (1995). Mapping the distribution of Golgi enzymes involved in the construction of complex oligosaccharides. J. Cell Sci. *108*, 1617–1627.

Rambourg, A., and Clermont, Y. (1990). Three-dimensional electron microscopy: structure of the Golgi apparatus. Eur. J. Cell Biol. *51*, 189–200.

Rothman, J.E., and Wieland, F.T. (1996). Protein sorting by transport vesicles. Science *272*, 227–234.

Sarras, M.P., Jr., Meador, D., and Zhang, X.M. (1991). Extracellular matrix (mesoglea) of Hydra vulgaris. II. Influence of collagen and proteoglycan components on head regeneration. Dev. Biol. *148*, 495–500.

Schekman, R., and Orci, L. (1996). Coat proteins and vesicle budding. Science *271*, 1526–1533.

Schekman, R., and Mellman, I. (1997). Does COPI go both ways? Cell *90*, 197–200.

Schmelz, M., Sodeik, B., Ericsson, M., Wolffe, E.J., Shida, H., Hiller, G., Griffiths, G. (1994). Assembly of vaccinia virus: the second wrapping cisterna is derived from the trans Golgi network. J. Virol. *68*, 130–147.

Trelstad, R.L., and Hayashi, K. (1979). Tendon collagen fibrillogenesis: intracellular subassemblies and cell surface changes associated with fibril growth. Dev. Biol. *71*, 228–242.

Velasco, A., Hendricks, L., Moremen, K.W., Tulsiani, D.R., Touster, O., and Farquhar, M.G. (1993). Cell type-dependent variations in the subcellular distribution of alpha-mannosidase I and II. J. Cell Biol. *122*, 39–51.